Coordination Polymers

DOI: 10.1002/ange.201202285

# An Alkaline Earth $I^3O^0$ Porous Coordination Polymer: $[Ba_2TMA(NO_3)(DMF)]$**

*Maw Lin Foo, Satoshi Horike, Yasutaka Inubushi, and Susumu Kitagawa**

Porous Coordination Polymers (PCPs) or Metal-Organic Frameworks (MOFs) are an emerging class of microporous solids combining the modularity of inorganic structural building units (nodes) with organic ligands (linkers) that can be tailored through organic synthesis.[1] This particular combination of designability and the structural porosity of PCPs has led to explosive growth in their application to gas storage/separation, catalysts, ion conductivity, and drug delivery systems.[2]

From a review by Cheetham et al.,[3] the structure of PCPs/MOFs can be classified by the dimensionality of their inorganic and organic connectivity, $I^mO^n$ ($n,m = 0$, 1, 2, or 3). Where "I" refers to the dimensionality of the inorganic connectivity, as embodied by metal-oxygen-metal (M-O-M) bonds, and "O" refers to the connectivity of the organic component, the M-ligand-M bonds. Most PCP/MOFs, such as the archetypal framework $[Zn_4O(1,4\text{-BDC})_6]$ (MOF-5; $H_2BDC$ = benzenedicarboxylic acid),[4] can be classified as $I^0O^3$. This indicates that no extended M-O-M bonds are present and organic ligands bridge isolated metal centers in all three dimensions of the crystal structure. With regards to the inorganic connectivity, frameworks possessing higher dimensionality ($I^1O^n$, $I^2O^n$, and especially $I^3O^n$) are postulated to have enhanced thermal, chemical, and magnetic properties owing to the higher stability of the M-O-M linkages and the cooperative interactions between metal centers through bridging oxygens, as embodied by transition metal oxides. For example, [M(OH)(1,4-BDC)] (MIL-53; M = Al,[5] Ga,[6] In,[7] Fe,[8] Cr[9]) is an $I^1O^2$ framework with good thermal and chemical stability, as compared to MOF-5. However, it should be noted that the synthesis of porous frameworks having higher inorganic connectivity, such as $I^3O^n$, is still a significant challenge.

It has been observed that with first row transition metals (especially nickel), such frameworks may be assembled with aliphatic dicarboxylates. This is probably due to the higher degree of flexibility of aliphatic ligands, as compared to their aromatic counterparts. Nickel succinate,[10] the first $I^3O^0$ framework synthesized, is thermally stable up to 698 K, which is a high value for PCPs. This was quickly followed by nickel glutarate.[11] Another approach utilizes late main group elements, which possess a higher coordination number than early transition metals. This approach has been successful with aromatic carboxylic acids as ligands, as embodied by the framework $[Pb_5(1,3\text{-BDC})_5(H_2O)_2]$.[12] To the best of our knowledge, from the handful of $I^3O^n$ ($n = 0,1,2,3$) frameworks known,[10–13] only nickel glutarate[11] and nickel aspartate[13a] have been demonstrated to be unambiguously porous by nitrogen adsorption measurements. As for aliphatic dicarboxylate frameworks, although they are capable of reversible hydration/dehydration, they are also vulnerable to structural rearrangement/collapse under evacuation.[11] As aromatic rings are more rigid than aliphatic chains, $I^3O^n$ porous frameworks with aromatic rings should exhibit enhanced stability and physical properties. However, none has been reported thus far.

Our group has been exploring barium PCPs because, prior to our recent work,[14] no porous barium coordination polymers had been reported. Furthermore, the ionic radius of $Ba^{2+}$ (1.47 Å)[15] is larger than that of the lanthanides, and is the largest for stable Group II metals. The size of $Ba^{2+}$ ensures that a high coordination number with carboxylate oxygens will be adopted. A systematic increase in the inorganic connectivity of Group II PCPs with the same ligand has been previously demonstrated by Cheetham et al.[16] Thus, it should be possible to form porous barium $I^3O^n$ frameworks through the appropriate choice of an aromatic carboxylate ligand. Herein, we report the synthesis of $[Ba_2TMA(NO_3)(DMF)]\supset DMF$ ($[\mathbf{1}(DMF)]\supset DMF$), an alkaline earth $I^3O^0$ PCP framework constructed with trimesic acid ($H_3TMA$ = 1,3,5-benzenetricarboxylic acid). We note that another polymorph, non-porous $[Ba(HTMA)(H_2O)_2]\supset 0.5\,H_2O$ has been previously reported.[17] Framework **1** has three-dimensional

[*] Dr. M. L. Foo, Prof. Dr. S. Kitagawa
Japan Science and Technology Agency, ERATO
Kitagawa Integrated Pores Project
Kyoto Research Park Bldg #3, Shimogyo-ku, Kyoto 600-8815 (Japan)
and
Institute for Integrated Cell-Material Sciences (WPI-iCeMS)
Kyoto University, Yoshida, Sakyo-ku, Kyoto 606-8501 (Japan)
Dr. S. Horike, Prof. Dr. S. Kitagawa
Department of Synthetic Chemistry and Biological Chemistry,
Graduate School of Engineering, Kyoto University
Katsura, Nishikyo-ku, Kyoto, 615-8510(Japan)
Dr. S. Horike
Japan Science and Technology Agency, PRESTO
4-1-8 Honcho, Kawaguchi, Saitama 332-0012 (Japan)
Y. Inubushi
Synthesis Research Laboratory, Kurashiki Research Center
Kuraray Co.Ltd., 2045-1, Sakazu, Kurashiki, Okayama 710-0801 (Japan)

[**] This work was supported by the Japan Science and Technology Agency ERATO program and Grants-in-Aid for Scientific Research, the Japan Society for the Promotion of Science (JSPS) and the Japan Science and Technology Agency PRESTO program. The iCeMS is supported by the World Premier International Research Initiative (WPI), MEXT (Japan). We thank Dr. Charlotte Bonneau for topology calculations and Dr. Yuh Hijikata for adsorption energy calculations. DMF = dimethylformamide, $H_3TMA$ = trimesic acid.

Supporting information for this article is available on the WWW under http://dx.doi.org/10.1002/anie.201202285.

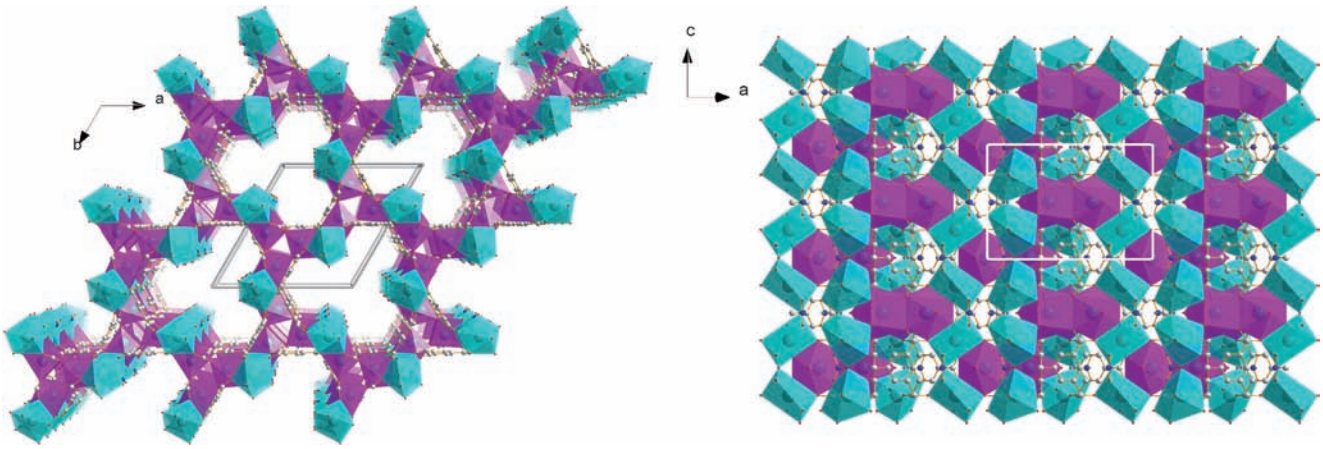


***Figure 1.*** Crystal structure of $[Ba_2TMA(NO_3)(DMF)]$ ($3\times3\times3$ unit cells). (left) View along the *c* axis with emphasis on the Ba1–$O_9$ polyhedron (magenta) and Ba2–$O_8$ polyhedron (cyan). One unit cell is outlined in gray. Gray spheres represent carbon, red spheres represent oxygen, and blue spheres represent nitrogen. Hydrogens and non-oxygen portions of coordinated DMF have been omitted for clarity. (right) View along the *b* axis showing the connectivity of Ba–O polyhedra by corner and edge sharing. The $Ba_9O_{54}$ repeating cluster used for topological calculations is outlined in white.

barium-oxygen-barium bonding with one-dimensional channels decorated by protruding oxygen atoms. The porosity of [**1**(acetone)] has been unequivocally demonstrated by $N_2$ gas adsorption measurements.

By combining $Ba(NO_3)_2$, $H_3TMA$, and DMF at 423 K, colorless needles were obtained, and the structure of the product was elucidated by single crystal X-ray diffraction. The structure of [**1**(DMF)]⊃DMF was solved in the non-centrosymmetric $P\bar{6}2c$ space group (190). In the asymmetric unit, there are two crystallographically distinct $Ba^{2+}$ cations (Ba1 and Ba2), one fully deprotonated $TMA^{3-}$ anion, one bridging $NO_3^-$ anion, and one coordinated DMF molecule, which gives a molecular formula of $[Ba_2TMA(NO_3)(DMF)]$.

The structure of **1** can be simply described as Ba2 ions (5.129 Å apart) forming one-dimensional chains along the *c* axis interspersed with equilateral triangles of Ba1 ions (4.243 Å apart) along the *ab* plane. There is one coordinated DMF molecule for each Ba1. The Ba ions are connected through TMA ligands with each carboxylate group binding three Ba ions in a *syn-syn-syn* manner. Each nitrate ligand is tetradentate and connects two Ba2 ions with $C_{2v}$ symmetry. If one considers the Ba–O polyhedra in **1** (Figure 1), it is observed that they are linked in all three dimensions by corner (Ba2–Ba2) and edge sharing (Ba1–Ba1 and Ba1–Ba2) to afford one-dimensional channels along the *c* axis comprised of three Ba2–$O_8$ and twelve Ba1–$O_9$ polyhedra. The TMA ligands line the pore channels in the fashion of a 2D kagome net.[18] Because of the connectivity of its Ba–O polyhedra, **1** can be classified as an $I^3O^0$ PCP.

The three-leaf-clover-shaped (three-fold symmetric) channels of **1** (Figure 2) are reminiscent of the zeolite cloverite,[19] which has four-leaf-clover-shaped channels. The pore dimension of each channel in **1** is approximately 13 Å at its widest point, but is restricted to 6.5 Å at its narrowest segment. Owing to bridging nitrates, the pores of **1** are lined with protruding oxygen atoms (Figure 2).

The trimesic anion is on a *c*-glide plane with a perpendicular mirror plane bisecting the molecule. The bonding mode

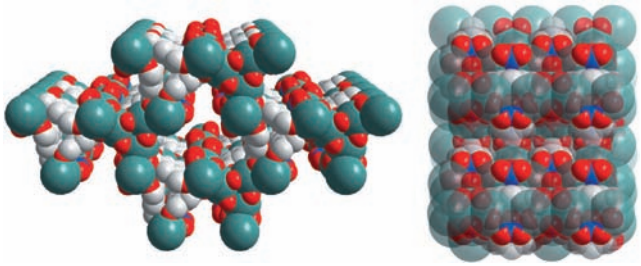

***Figure 2.*** Pore channels. (left) View of **1** along the *c* axis showing protruding oxygen atoms (red) lining the pore channels. Dark green spheres represent barium, blue spheres represent nitrogen, and gray spheres represent carbon. (right) Longitudinal view of pore channels with emphasis on the nitrate anion.

of all the carboxylates are identical and can be described as $\mu^3$-$\eta^2$:$\eta^1$:$\eta^2$ (each carboxylate group binds to a total of three metal atoms and each oxygen of the carboxylate group is coordinated to two metal atoms). This is in accordance with the previous literature on CPs synthesized with heavy metals, such as Pb, Cd, and the lanthanides.[20] The equivalent description for the nitrate anion is $\mu^2$-$\eta^2$: $\eta^2$. This mode of bonding has previously been observed only in non-porous coordination polymers.[21]

Ba1 on a mirror plane is nine-coordinated (Figure 3) with eight carboxylate oxygen atoms (O2, O2A, O2B, O2C, O3, O3A, O6, O6A) from three carboxylates and one coordinated DMF molecule (O1). The Ba–O bond distances vary from 2.724–2.955 Å, with the longest bond from the coordinated solvent. Ba1 forms a unique equilateral triangular motif, $Ba_3(-CO_2)_9(DMF)_3$, which has not been previously observed in other barium coordination compounds. As each $Ba^{2+}$ ion is coordinated to one DMF, three potential open metal sites are available for each motif. Although somewhat similar to the ubiquitous $M_3O(-CO_2)_6$ (where M is typically $Ru^{2+/3+}$, $Fe^{2+/3+}$, $Cr^{3+}$)[22] structural building unit (SBU) where three potential open metal sites are also available, two important structural

  

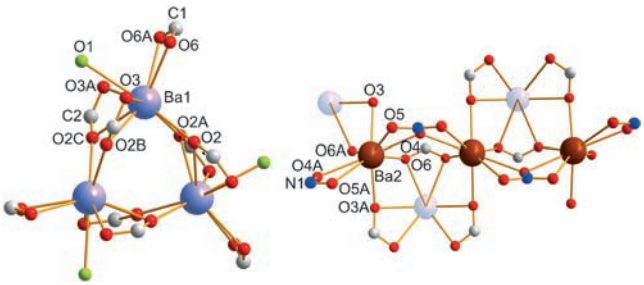


***Figure 3.*** Coordination environments of Ba. (left) The Ba1 trimeric unit. Lavender spheres represent Ba1, gray spheres represent carbon, red spheres represent oxygen, lime spheres represent oxygen from coordinated DMF. (right) The one-dimensional Ba2 chains. Brown spheres represent Ba2 and blue spheres represent nitrogen.

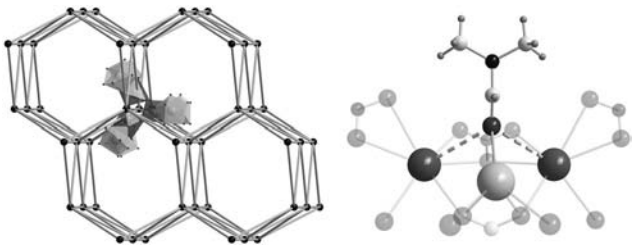

***Figure 4.*** Topology of **1** and coordination environment of DMF. (left) Topological simplification of **1** by an eight-connected uninodal **eca** net. Superimposed on one of the nodes is a repeating $Ba_9O_{54}$ cluster. (right) Coordination environment of bound DMF between Ba1 (light gray) and Ba2 (dark gray). Weak interactions between Ba2 and the carbonyl oxygen is shown with dotted lines.

differences are present: 1) A $\mu^3$-oxo connecting all three barium centers is absent, in comparison with the $M_3O(-CO_2)_6$ SBU. 2) Carboxylates with a $\mu^2$-$\eta^1$:$\eta^1$ bonding mode are found in the $M_3O(-CO_2)$ SBU, but in $Ba_3(-CO_2)_9(DMF)_3$, a $\mu^3$-$\eta^2$:$\eta^1$:$\eta^2$ bonding mode is present, which implies that there is bonding to atoms outside the triangular motif (for example, to Ba2), thus precluding it from being referred to as a SBU.

Ba2 on a two-fold rotation axis forms one-dimensional chains running along the *c* axis (Figure 3), although the distance between two adjacent Ba2 centers is too far (5.129 Å) for direct bonding to occur. Instead, they are interconnected by carboxylates and bridging nitrates. Ba2 is eight-coordinated with four oxygen atoms from individual carboxylates (O3, O3A, O6, O6A) and four oxygen atoms (O4, O4A, O5, O5A) from two nitrate anions. The Ba–O bond distances vary from 2.699 to 2.934 Å, with the longest bond to the nitrate anion. For each Ba2, there are potentially two extra "bonds" to O1, the carbonyl oxygen of the coordinated DMF molecule. However, owing to the long $Ba–O_{carbonyl}$ distance (3.189 Å), which is unprecedented, and for simplification of the structure, we have chosen to represent the structure of **1** without any formal bonds from Ba2 to O1.

The topology of **1** is obtained by considering the inorganic portion of the framework only, as both the TMA and nitrate ligands are completely surrounded by Ba–O bonds. The node is defined by a repeating $Ba_9O_{54}$ cluster (Figures 2 and 4) with site symmetry $\bar{6}m2$ at (2/3, 1/3, 1/4). Each $Ba_9O_{54}$ cluster consists of one $(Ba1)_3O_{21}$ triangular motif (formed by edge sharing Ba1–$O_9$ polyhedra) surrounded by three edge sharing $(Ba2)_2O_{15}$ subunits. The $(Ba2)_2O_{15}$ subunit consists of a pair of corner-sharing Ba2–$O_8$ polyhedra. In the *ab* plane, each cluster is connected to six others, with one above and one below, making the cluster eight coordinated (Figure 4). Evaluation of the network by Systre[23] reveals that the topology is a rare **eca** (RCSR notation) net.[24] Such a topology, to the best of our knowledge, has not been previously observed in PCPs, unlike other eight-coordinated nets, such as **bcu**[25] or **hex**.[26] As the site symmetry of the net matches that of the cluster, the choice of abstraction is verified.

Thermogravimetric analysis (TGA) on [**1**(DMF)]⊃DMF under a flow of $N_2$ at 973 K shows a three step isotherm. The first step is the loss of 0.9 DMF molecule/formula unit in the pores (actual 9.61 %, calculated 9.64 %) from room temperature to 623 K, followed by the loss of one coordinated DMF molecule/formula unit (actual 10.56 %, theoretical 10.70 %) to ca. 753 K, and finally, decomposition of the compound. Thus, [**1**(DMF)]⊃0.9 DMF is the molecular formula of the compound. Separate heating experiments with XRD under vacuum verify that the structure of **1** is still intact at 698 K, indicating that the high thermal stability of the compound is due to three-dimensional Ba-O-Ba bonding. Even in air, the crystallinity of the framework is retained until 623 K. In comparison, $[Ba(HTMA)(H_2O)_2]⊃0.5\,H_2O$, an $I^1O^2$ framework with the same metal and ligand, is only thermally stable until 558 K in $N_2$.[17] This result demonstrates the superior stability of a PCP with a three-dimensionally connected inorganic framework.

The porosity of **1** is estimated to be 34.3 % using PLATON software. To test this, attempts were made to measure the gas adsorption properties of the polymer. All attempts to heat [**1**(DMF)]⊃DMF at 373–698 K under evacuation for nitrogen adsorption measurements did not result in measurable surface areas. From IR measurements, the carbonyl peak from coordinated DMF persists even at 623 K and was finally removed at 698 K, in accordance with the TGA profile. Although each coordinated DMF is primarily bound to Ba1, there are two Ba2 ions within 3.189 Å, as mentioned previously. Thus, the coordinated DMF is bound by its carbonyl oxygen in a pseudo-$\mu^3$-bridging mode rather than a $\mu^1$-bridging mode (Figure 4). As the structure is stable until 698 K, as evidenced by XRD, the absence of significant surface area is probably due to decomposition of bound DMF within the pores, as indicated by the samples turning brown.

To lower the temperature of evacuation, [**1**(DMF)]⊃DMF was exchanged with acetone. Powder XRD shows that the structure of [**1**(acetone)]⊃acetone is unchanged. The complete exchange of DMF for acetone was verified by a shift of the carbonyl band from 1651 to 1699 $cm^{-1}$. The downward shift of the carbonyl band in acetone from 1714 $cm^{-1}$ (liquid) to 1699 $cm^{-1}$ (coordinated) is an indication of a strong Lewis acidic environment, which is created by the Ba1-Ba2-Ba2 triangle shown in Figure 4. The TGA of the exchanged framework is very similar to that of the as-synthesized compound, except for an initial weight loss at $<373$ K,

  

indicating that acetone is more easily lost than DMF from the pores. From TGA, the formula of the acetone exchange compound was determined to be [**1**(acetone)]⊃0.8 acetone.

Evacuation of [**1**(acetone)]⊃acetone at 358 K removed unbound acetone and afforded [**1**(acetone)], which is a porous compound with a Langmuir surface area of 235 $m^2 g^{-1}$ (BET surface area = 190 $m^2 g^{-1}$; Figure 5), as determined by nitrogen adsorption measurements at 77 K.

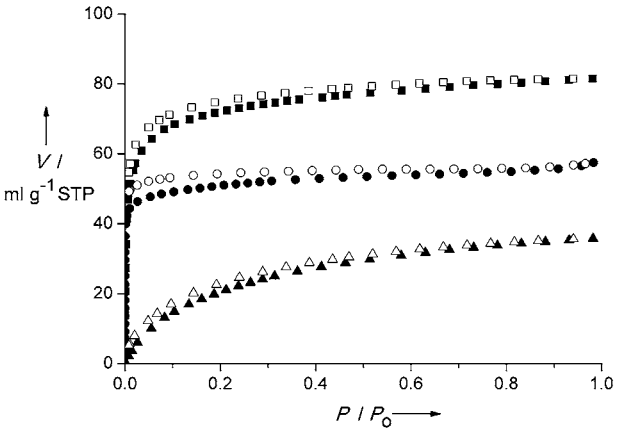


***Figure 5.*** Gas adsorption isotherms of [**1**(acetone)] for $CO_2$ at 195 K (■/□), $N_2$ at 77 K (●/○), and $CH_4$ at 195 K (▲/△). Filled and empty characters represent adsorption and desorption, respectively.

The presence of coordinated acetone remaining after gas adsorption measurements was confirmed by IR analysis. Thus, [**1**(acetone)] is the first PCP with an $I^3O^0$-type structure that is constructed with aromatic ligands. As with the as-synthesized compound, all attempts to remove the bound acetone coordinated to the barium centers by heating under evacuation were unsuccessful before decomposition. It is postulated that this is due to a combination of the unique pore geometry of the PCP and strong binding from the barium centers.

$CO_2$ and $CH_4$ gas adsorption measurements were undertaken at 195 K to examine the ability of [**1**(acetone)] to separate these two gases. As evidenced by the gas adsorption isotherms, $CO_2$ is preferably adsorbed, especially at low pressures ($P/P_0 = 0.2$; $V(CO_2) = 70\,mL\,g^{-1}$ and $V(CH_4) = 20\,mL\,g^{-1}$ at STP). This selectivity is predominantly due to a molecular sieving effect[27] owing to the pore size and geometry of [**1**(acetone)], as the heat of adsorption for $CO_2$ is only moderately high (25–29 $kJ\,mol^{-1}$). Because of this result, high pressure measurements were performed at 273 K, which confirmed the favorable adsorption of $CO_2$. We then proceeded to conduct breakthrough experiments, as they can evaluate the gas separation ability of adsorbents under kinetic flowing gas conditions, which are pertinent to the pressure swing adsorption (PSA) process used in industry. Upon initial injection of the $CH_4/CO_2$ (60:40 v/v) gas mixture (Figure 6), the concentration of $CO_2$ detected by gas chromatography (GC) was 0% and $CH_4$ 100% until the breakpoint at ca. 10 min. As complete separation was achieved, [**1**(acetone)] can potentially be used for $CO_2$ separation, both under gas equilibrium conditions and under gas flow conditions.

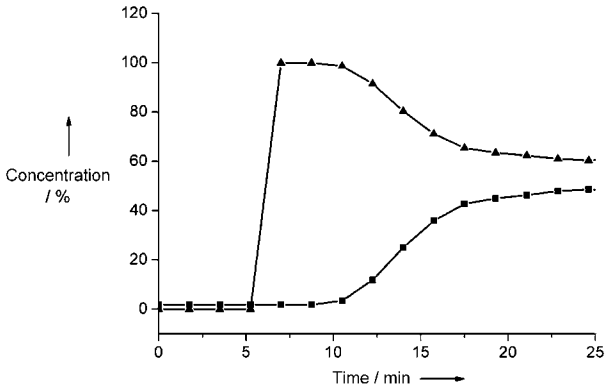


***Figure 6.*** Breakthrough curves of [**1**(acetone)] for a mixture of $CH_4/CO_2$ (60:40 v/v) at 0.8 MPa with 6 $min^{-1}$ space velocity at 273 K. $CH_4$ (▲), $CO_2$ (■).

In conclusion, the combination of permanent porosity, three-dimensionally connected barium-oxide-barium centers in a previously unobserved **eca** net, a new trimeric motif with potential open metal (Lewis acidic) sites, and bridging nitrates (Lewis basic sites) combine to make **1** a unique main group PCP. The compound can be classified as an $I^3O^0$-type framework, and is the first example to have permanent porosity constructed from an aromatic carboxylate ligand. The use of $Ba^{2+}$, which has a large ionic radius, and a small aromatic ligand (TMA) is crucial for the construction of this porous $I^3O^0$ compound. We have shown that [**1**(acetone)] is capable of $CO_2/CH_4$ separation in both equilibrium gas adsorption and breakthrough setup and we are currently exploring other applications of this unique PCP.

## *Experimental Section*

[$Ba_2$TMA$(NO_3)$(DMF)]⊃DMF ([**1**(DMF)]⊃DMF): $Ba(NO_3)_2$ (104.5 mg or 0.4 mmol; Wako) was added to trimesic acid (42.0 mg, 0.2 mmol; TCI) in DMF (20 mL) in a glass vial with a volume of 30 mL. The vial was then sealed with a Teflon-lined cap and heated to 140 °C for 24 h to obtain colorless needles (10–40 μm in length). The mixture was filtered and washed with DMF (10 mL), $CH_2Cl_2$ (1 mL) and then briefly air-dried to afford the product (83.2 mg; 67% with respect to ligand). Elemental Analysis: calculated for [$Ba_2$TMA$(NO_3)$(DMF)]⊃0.3 DMF ($C_{12}H_{10}N_2O_{10}Ba_2$–0.3 $C_3H_7NO$): C, 24.25; H, 1.91; N, 5.04; Found: C 24.33; H, 1.88; N, 4.99. The difference in the number of DMF molecules, as determined by TGA and elemental analysis, is because of the loss of DMF molecules during analysis. Larger single crystals can be obtained, at the expense of yield, by employing identical conditions and lowering the ratio of metal/ligand from 2:1 to 1:1. A crystal synthesized from a metal/ligand ratio of 1:1 was used for single crystal X-ray diffraction.

Crystal data: Single crystal X-ray diffraction measurements were performed at 223 K with a Rigaku AFC10 diffractometer with Rigaku Saturn Kappa CCD system equipped with a MicroMax-007 HF/VariMax rotating-anode X-ray generator with confocal monochromated $MoK_\alpha$ radiation (0.71075 Å) operating at 50 kV and 24 mA. Data were processed using Crystal Clear TM-SM (Version 1.4.0). The crystal structure was solved by a direct method and refined by full matrix least squares refinement against $|F|^2$ using SHELXL-97. To obtain a suitable refinement with coordinated DMF, restraints were placed on bond distances of the DMF molecule between C7–O1, C7–N2, and N2–C8. C7, C8, and N2 were refined isotropically owing to

their large thermal vibrations, and all the rest of the non-hydrogen atoms were refined anisotropically. N1 and O5 from the bridging nitrate possess strong thermal anisotropy along the channel direction (*c* axis). Hydrogen atoms were placed in calculated positions with isotropic U values 20% higher than the atom to which they were bound. CCDC 872673 contains the supplementary crystallographic data for this paper. These data can be obtained free of charge from The Cambridge Crystallographic Data Centre via www.ccdc.cam.ac.uk/data_request/cif.

Crystal data for [**1**(DMF)]⊃DMF ([$C_{12}H_{10}Ba_2N_2O_{10}$]⊃DMF): Hexagonal, $P\bar{6}2c$ (190), $a = 17.8254(4)$, $c = 10.2582(2)$ Å, $V = 2823(1)$ Å$^3$, $Z = 6$, $\rho = 2.177$ g cm$^{-3}$. $R_1 = 0.0260$ ($I > 2\sigma$) for 2284 unique reflections with 121 parameters, 3 restraints. GoF = 1.085, Flack parameter = 0.02(3). Largest difference peak and hole: 0.939 and −0.779 electron Å$^{-3}$.

Received: March 23, 2012
Published online: May 8, 2012

**Keywords:** barium · carbon dioxide · coordination compounds · hybrid materials · porosity

[1] a) S. Kitagawa, R. Kitaura, S. Noro, *Angew. Chem.* **2004**, *116*, 2388 – 2430; *Angew. Chem. Int. Ed.* **2004**, *43*, 2334 – 2375; b) J. L. C. Rowsell, O. M. Yaghi, *Microporous Mesoporous Mater.* **2004**, *73*, 3 – 14; c) H.-C. Zhou, J. R. Long, O. M. Yaghi, *Chem. Rev.* **2012**, *112*, 673 – 674 (feature issue).

[2] a) R. J. Kuppler, D. J. Timmons, Q. R. Fang, J. R. Li, T. A. Makal, M. D. Young, D. Q. Yuan, D. Zhao, W. J. Zhuang, H. C. Zhou, *Coord. Chem. Rev.* **2009**, *253*, 3042 – 3066; b) L. Q. Ma, C. Abney, W. B. Lin, *Chem. Soc. Rev.* **2009**, *38*, 1248 – 1256; c) A. C. McKinlay, R. E. Morris, P. Horcajada, G. Ferey, R. Gref, P. Couvreur, C. Serre, *Angew. Chem.* **2010**, *122*, 6400 – 6406; *Angew. Chem. Int. Ed.* **2010**, *49*, 6260 – 6266.

[3] A. K. Cheetham, C. N. R. Rao, R. K. Feller, *Chem. Commun.* **2006**, 4780 – 4795.

[4] H. Li, M. Eddaoudi, M. O'Keeffe, O. M. Yaghi, *Nature* **1999**, *402*, 276 – 279.

[5] T. Loiseau, C. Serre, C. Huguenard, G. Fink, F. Taulelle, M. Henry, T. Bataille, G. Férey, *Chem. Eur. J.* **2004**, *10*, 1373 – 1382.

[6] C. Volkringer, T. Loiseau, N. Guillou, G. Ferey, E. Elkaim, A. Vimont, *Dalton Trans.* **2009**, 2241 – 2249.

[7] E. V. Anokhina, M. Vougo-Zanda, X. Wang, A. J. Jacobson, *J. Am. Chem. Soc.* **2005**, *127*, 15000 – 15001.

[8] C. Scherb, A. Schödel, T. Bein, *Angew. Chem.* **2008**, *120*, 5861 – 5863; *Angew. Chem. Int. Ed.* **2008**, *47*, 5777 – 5779.

[9] C. Serre, F. Millange, C. Thouvenot, M. Noguès, G. Marsolier, D. Louër, G. Férey, *J. Am. Chem. Soc.* **2002**, *124*, 13519 – 13526.

[10] P. M. Forster, A. K. Cheetham, *Angew. Chem.* **2002**, *114*, 475 – 477; *Angew. Chem. Int. Ed.* **2002**, *41*, 457 – 459.

[11] N. Guillou, C. Livage, M. Drillon, G. Férey, *Angew. Chem.* **2003**, *115*, 5472 – 5475; *Angew. Chem. Int. Ed.* **2003**, *42*, 5314 – 5317.

[12] L. Zhang, Z.-J. Li, Q.-P. Lin, Y.-Y. Qin, J. Zhang, P.-X. Yin, J.-K. Cheng, Y.-G. Yao, *Inorg. Chem.* **2009**, *48*, 6517 – 6525.

[13] a) E. V. Anokhina, Y. B. Go, Y. Lee, T. Vogt, A. J. Jacobson, *J. Am. Chem. Soc.* **2006**, *128*, 9957 – 9962; b) R. Vaidhyanathan, S. Natarajan, C. N. R. Rao, *Dalton Trans.* **2003**, 1459 – 1464; c) C. Livage, P. M. Forster, N. Guillou, M. M. Tafoya, A. K. Cheetham, G. Férey, *Angew. Chem.* **2007**, *119*, 5981 – 5983; *Angew. Chem. Int. Ed.* **2007**, *46*, 5877 – 5879; d) L. N. Appelhans, M. Kosa, A. V. Radha, P. Simoncic, A. Navrotsky, M. Parrinello, A. K. Cheetham, *J. Am. Chem. Soc.* **2009**, *131*, 15375 – 15386.

[14] M. L. Foo, S. Horike, S. Kitagawa, *Inorg. Chem.* **2011**, *50*, 11853 – 11855.

[15] R. Shannon, *Acta Crystallogr. Sect. A* **1976**, *32*, 751 – 767.

[16] E. H. L. Falcão, Naraso, R. K. Feller, G. Wu, F. Wudl, A. K. Cheetham, *Inorg. Chem.* **2008**, *47*, 8336 – 8342.

[17] M. J. Plater, A. J. Roberts, J. Marr, E. E. Lachowski, R. A. Howie, *J. Chem. Soc. Dalton Trans.* **1998**, 797 – 802.

[18] I. Syôzi, *Prog. Theor. Phys.* **1951**, *6*, 306 – 308.

[19] M. Estermann, L. B. McCusker, C. Baerlocher, A. Merrouche, H. Kessler, *Nature* **1991**, *352*, 320 – 323.

[20] a) A. Morsali, A. R. Mahjoub, *Helv. Chim. Acta* **2004**, *87*, 2717 – 2722; b) Y.-P. Yuan, J.-L. Song, J.-G. Mao, *Inorg. Chem. Commun.* **2004**, *7*, 24 – 26; c) S. Wang, L. Zhang, G. Li, Q. Huo, Y. Liu, *CrystEngComm* **2008**, *10*, 1662 – 1666.

[21] A. Schuy, H. Billetter, F. Hohn, I. Pantenburg, U. Ruschewitz, *Z. Kristallogr.* **2005**, *220*, 250 – 258.

[22] D. J. Tranchemontagne, J. L. Mendoza-Cortes, M. O'Keeffe, O. M. Yaghi, *Chem. Soc. Rev.* **2009**, *38*, 1257 – 1283.

[23] O. Delgado-Friedrichs, M. O'Keeffe, *Acta Crystallogr. Sect. A* **2003**, *59*, 351 – 360.

[24] I. Baburin, V. Blatov, *Russ. J. Inorg. Chem.* **2007**, *52*, 1577 – 1585.

[25] D.-L. Long, A. J. Blake, N. R. Champness, C. Wilson, M. Schröder, *Angew. Chem.* **2001**, *113*, 2509 – 2513; *Angew. Chem. Int. Ed.* **2001**, *40*, 2443 – 2447.

[26] L. Pan, H. Liu, X. Lei, X. Huang, D. H. Olson, N. J. Turro, J. Li, *Angew. Chem.* **2003**, *115*, 560 – 564; *Angew. Chem. Int. Ed.* **2003**, *42*, 542 – 546.

[27] T. Loiseau, L. Lecroq, C. Volkringer, J. Marrot, G. Férey, M. Haouas, F. Taulelle, S. Bourrelly, P. L. Llewellyn, M. Latroche, *J. Am. Chem. Soc.* **2006**, *128*, 10223 – 10230.

  